Spectroscopy of Gd^{3+} in KYF_4: a system with several luminescent sites

1991 J. Phys.: Condens. Matter 3 8959

(http://iopscience.iop.org/0953-8984/3/45/017)

J. Phys.: Condens. Matter 3 (1991) 8959–8966. Printed in the UK

Spectroscopy of Gd^{3+} in KYF_4: a system with several luminescent sites

J Sytsma†, S J Kroes†, G Blasse† and N M Khaidukov‡

† Debye Research Institute, University of Utrecht, PO Box 80.000, 3508 TA Utrecht, The Netherlands

‡ Institute of General and Inorganic Chemistry, USSR Academy of Sciences, Leninskii Prospekt 31, 117907 Moscow, USSR

Received 6 June 1991

Abstract. The spectroscopy of Gd^{3+} in KYF_4 is reported. Evidence is given that there are two different classes of luminescent sites: classes I and II. The positions of the crystal field components of the $^6P_{7/2}$ and $^6I_{7/2}$ term levels are presented. The radiative transition probabilities for the $^6P_{7/2} \rightarrow {}^8S_{7/2}$ transition are derived, for both classes, from decay measurements and spectral intensity measurements. At 4.2 K energy transfer occurs from class I to class II. Above 25 K energy transfer also occurs from class II to class I.

1. Introduction

Rare earth fluorides are important materials. Due to their chemical and physical properties they are advantageous materials for application in laser systems. Several reviews exist on the chemistry of the rare earth fluorides [1, 2]. Among the fluorides, KYF_4 has been classified as a prospective laser material [3]; in fact, KYF_4 doped with Nd^{3+} has been shown to be a promising laser material [4].

In this article we study the spectroscopic properties of KYF_4 doped with 5 at.% Gd^{3+}. The positions of the lowest term levels are presented. It is shown that there are two different classes of luminescent sites, which are labelled class I and class II. The liquid helium temperature values of the transition probabilities of transitions starting at the lowest crystal field components of the $^6P_{7/2}$ and the $^6I_{7/2}$ term levels are derived from the spectral data and decay measurements. At 4.2 K energy transfer occurs from class I to class II. Above 25 K energy transfer occurs also from class II to class I.

2. Experimental details

2.1. Sample preparation

The crystals were grown by hydrothermal synthesis. The size of the crystals is about 4 mm × 3 mm × 3 mm. The optical quality is good: the crystals are colourless and fully transparent. According to Greis and Haschke, KYF_4 is isostructural with $KErF_4$ ([2] and references therein). The structural analysis of $KErF_4$ has been performed by Aleonard *et al* [5]. This structure is related to the fluorite structure [2, 5]. The

0953-8984/91/458959+08$03.50

hexagonal unit cell contains three cation layers, stacked according the sequence 'abc'. In each layer there are twelve cation positions. Four of these positions are occupied by Y^{3+} in each layer. Another four positions are occupied by either Y^{3+} or K^+, according to a statistical distribution of four Y^{3+} ions and eight K^+ ions over the three layers. The last four positions are also occupied by either Y^{3+} or K^+, according to a statistical distribution of two Y^{3+} ions and ten K^+ ions over the three layers. The space group of the unit cell is $P3_112$ [5]. None of the cation positions has inversion symmetry [6].

The concentration of Gd^{3+} is 5 at.%.

2.2. Optical instrumentation

The measurements are performed with a frequency-doubled dye laser, pumped by a Nd–YAG laser (for details see [7]). The monochromator is a Spex 1269. Low resolution spectra are measured with a Perkin–Elmer MPF 44-B spectrofluorometer described in detail in [8]. During the measurements the temperature of the sample can be varied between 1.5 and 300 K.

3. Results

After laser excitation at 4.2 K at 35741 cm^{-1}, the lowest $^6I_{7/2}$ crystal field (CF) component, emission is observed in the $^6P_{7/2} \rightarrow {}^8S_{7/2}$ transition region (figure 1). The emission maxima are at 31987 and 32070 cm^{-1}. The emission line at 31987 cm^{-1} shows a pronounced shoulder on the higher energy side. We will not distinguish the shoulder from the main line for reasons mentioned later. After excitation into one of the higher $^6I_{7/2}$ CF components, at 35878 cm^{-1}, emission can also be observed in the $^6I_{7/2} \rightarrow {}^8S_{7/2}$ region. The maxima are at 35702 and 35741 cm^{-1} (figure 2). The energy difference between the maxima is 83 and 39 cm^{-1} in figures 1 and 2, respectively. These values are too large to ascribe the occurrence of more than one line in figures 1 and 2 to a thermal population of the higher crystal field components of the $^6P_{7/2}$ and $^6I_{7/2}$ term levels, respectively. The linewidths of the emission lines are $\approx$ 13 cm^{-1} for the lines at 32070 (figure 1) and 35741 cm^{-1} (figure 2) and $\approx$ 20 cm^{-1} for the lines at 31987 (figure 1) and 35702 cm^{-1} (figure 2). This is much larger than the linewidths of the corresponding transitions of Gd^{3+} in the crystalline powders of LaF_3 and $LiYF_4$ [9] and in the single crystal $Cs_2NaGdCl_6$ [10, 11], namely $\approx$ 5 cm^{-1}. Therefore, we conclude that there are two classes of sites for the Gd^{3+} ion, which give rise to different energy level schemes. Each of the classes shows a considerable inhomogeneous broadening due to the statistical distribution of Y^{3+} and K^+ over the cation positions. The classes are labelled I and II as in figure 1.

The assignment of two classes is confirmed by the excitation spectra of the different emission lines. The excitation spectra in the $^8S_{7/2} \rightarrow {}^6P_{7/2}$ region are given in figure 3. The excitation spectrum of the emission line at 31987 cm^{-1} (class II) shows at least six lines (figure 3(*b*)). For a Gd^{3+} ion on a site without inversion symmetry the $^6P_{7/2}$ term level is expected to split into four CF components. Three of the lines, however, are also present in the excitation spectrum of the emission line at 32070 cm^{-1} (class I) (figure 3(*a*)). Therefore, we conclude that at 4.2 K energy transfer occurs from class I to class II, but not vice versa. A comparison of the two excitation spectra allows an assignment of the lines to the different CF components of the $^6P_{7/2}$ term level of Gd^{3+}

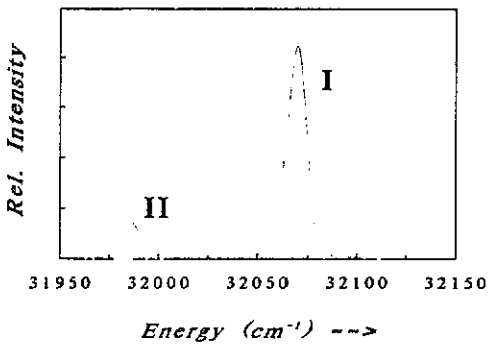

Figure 1. Emission spectrum in the $^6P_{7/2} \rightarrow {}^8S_{7/2}$ region of Gd^{3+} in KYF_4 at 4.2 K. Excitation at 35 741 cm^{-1}. The labels 'I' and 'II' define the class of site numbering.

Figure 2. Emission spectrum in the $^6I_{7/2} \rightarrow {}^8S_{7/2}$ region of Gd^{3+} in KYF_4 at 4.2 K. Excitation is at 35 878 cm^{-1}. The labels 'I' and 'II' indicate the class of sites.

in class I and class II as in figure 3. Lines occurring in both spectra are assigned to the CF components of the $^6P_{7/2}$ term level of Gd^{3+} in class I. The remaining lines in figure 3(b) are assigned to the CF components of the $^6P_{7/2}$ term level of Gd^{3+} in class II. The positions and assignments are tabulated in table 1. The total CF splitting of the $^6P_{7/2}$ term level of class I is estimated to be 84 cm^{-1}; the CF splitting of class II yields 167 cm^{-1}.

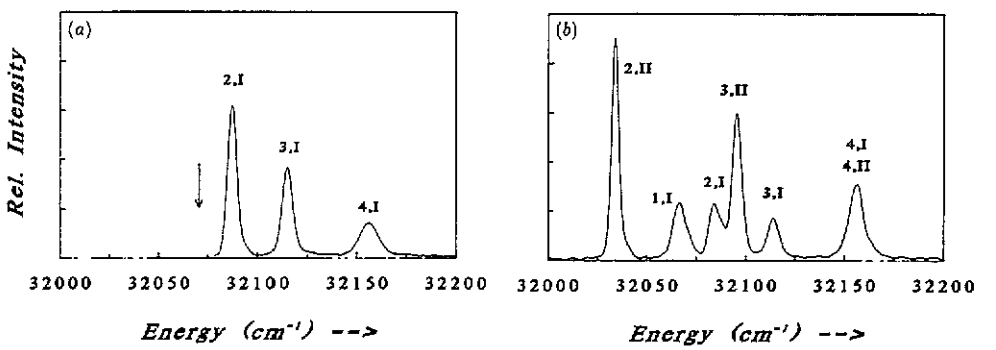

Figure 3. Excitation spectrum in the $^8S_{7/2} \rightarrow {}^6P_{7/2}$ region of the $^6P_{7/2} \rightarrow {}^8S_{7/2}$ transition of the two classes of sites of Gd^{3+} in KYF_4 at 4.2 K. (a) is for emission from class I. The arrow indicates the position of the monitored emission line. (b) is for emission from class II. The differences in intensity of the lines in (a) and (b) allow an assignment of the lines to class I or II. The lines are labelled with the CF component index and the class number.

The excitation spectrum of the emission at 32 005 cm^{-1}, i.e. the shoulder mentioned earlier, does not differ from the excitation spectrum of the main $^6P_{7/2} \rightarrow {}^8S_{7/2}$ emission line of class II (at 31 987 cm^{-1}). We therefore also classify the shoulder as class II emission.

Table 1. Data on the Gd^{3+} spectroscopy in KYF_4. Two classes of sites are observed (I and II). For both classes the following results are given: the positions of the $^6P_{7/2}$ and $^6I_{7/2}$ CF components, the ratio r of the vibronic intensity to the zero-phonon intensity for the $^6P_{7/2} \rightarrow {}^8S_{7/2}$ transition, and the transition probabilities at 4.2 K. The radiative transitions are to the $^8S_{7/2}$ ground state, whereas the non-radiative transitions of the $^6I_{7/2}$ term level are to the ^6P_J term levels. The error in the transition probabilities is about 10% and is mainly due to the error in the relative intensity measurements.

Class		I	II
$^6P_{7/2}^{(\mu)}$ (in cm^{-1})	$\mu = 1$	32070	31987
	$\mu = 2$	32082	31032
	$\mu = 3$	32113	32095
	$\mu = 4$	32154	32154
Barycentre (cm^{-1})		32105	32067
CF splitting (cm^{-1})		84	167
$r^{(\mu)} = r$		0.04	0.05
τ^{-1} (in ms)		9.2	9.5
$A_{zp}^{(1)}$ (in s^{-1})		105	100
$A_{vib}^{(1)}$ (in s^{-1})		4	5
$^6I_{7/2}^{(\mu)}$ (in cm^{-1})	$\mu = 1$	35741	35782
	$\mu = 2$	35787	35764
	$\mu = 3$	35845	35787
	$\mu = 4$	35878	35862
Barycentre (cm^{-1})		35813	35779
CF splitting (cm^{-1})		137	160
τ^{-1} (in ms)		2.8	2.6
$A_{zp}^{(1)}$ (in s^{-1})		259	279
$A_{nr}^{(1)}$ (in s^{-1})		98	106

The excitation spectra in the $^8S_{7/2} \rightarrow {}^6I_{7/2}$ region of the main $^6P_{7/2} \rightarrow {}^8S_{7/2}$ emission lines are given in figure 4. The two excitation spectra differ significantly. The lines at 35702, 35764 and 35862 cm^{-1} occurring in the excitation spectrum of class II, figure 4(*b*), do not occur in the excitation spectrum of class I, figure 4(*a*). The excitation spectra of the $^6I_{7/2} \rightarrow {}^8S_{7/2}$ emission line at 35702 cm^{-1} is equal to the excitation spectrum of the $^6P_{7/2} \rightarrow {}^8S_{7/2}$ emission line of class II. The excitation spectra of the $^6I_{7/2} \rightarrow {}^8S_{7/2}$ emission line at 35741 cm^{-1} is equal to the excitation spectrum of the $^6P_{7/2} \rightarrow {}^8S_{7/2}$ emission line of class I. The emission lines in the $^6I_{7/2} \rightarrow {}^8S_{7/2}$ region can thus be assigned to the two sites as in figure 2.

Now that we know that at 4.2 K energy transfer occurs from class I to class II and that the CF splitting of class II is the largest we are able to assign the lines in figure 4. The positions and assignments are tabulated in table 1. The total CF splitting of the $^6I_{7/2}$ term level of Gd^{3+} in class I (II) is 137 (160) cm^{-1}.

It is possible to excite class II selectively by tuning the excitation to 35702 cm^{-1}. A single emission line is now observed. The decay curve at 4.2 K shows a build up

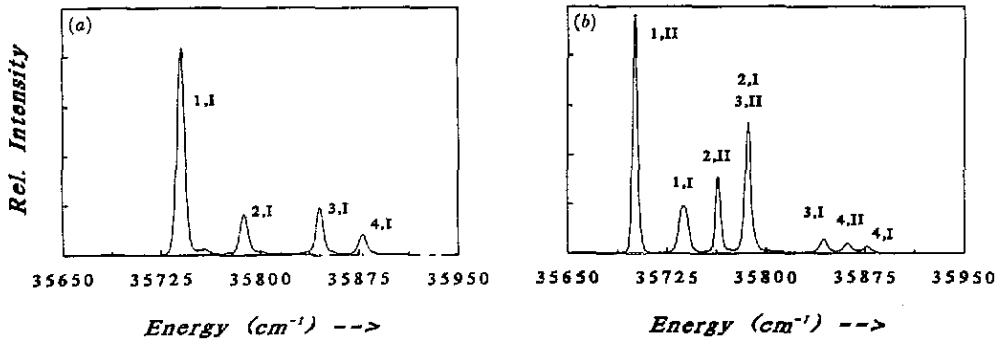

Figure 4. Excitation spectrum in the $^8S_{7/2} \rightarrow {}^6I_{7/2}$ region of the $^6P_{7/2} \rightarrow {}^8S_{7/2}$ emission of the two classes of sites of Gd^{3+} in KYF_4 at 4.2 K. (*a*) is for emission from class I, (*b*) is for emission from class II. The lines are labelled with the CF component index and the class number.

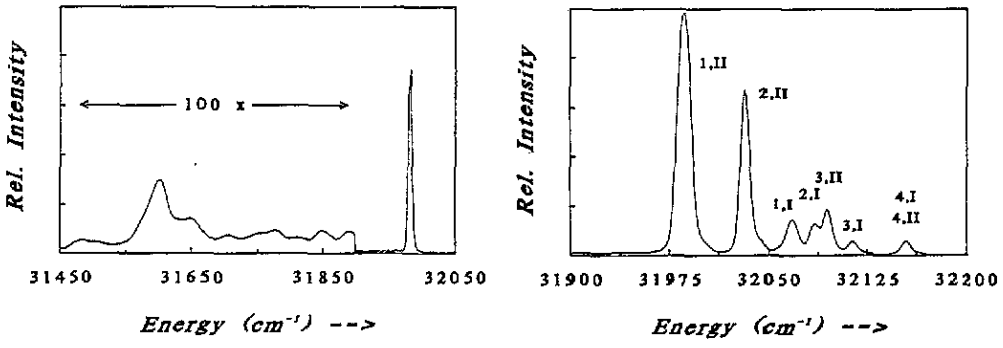

Figure 5. Emission spectrum of the $^6P^{(1)}_{7/2} \rightarrow {}^8S_{7/2}$ transition of Gd^{3+} in class II in KYF_4 at 4.2 K. Excitation is at 35 702 cm^{-1}. On the right-hand side of the spectrum is the zero-phonon line; at lower energies vibronic lines are observed.

Figure 6. Emission spectrum of the $^6P_{7/2} \rightarrow {}^8S_{7/2}$ transition of Gd^{3+} in KYF_4 at 62 K, after excitation at 35 702 cm^{-1}. Despite selective excitation of class II, emission is also observed from class I. The lines are labelled with the CF component index and the class number.

due to feeding from the $^6I^{(1)}_{7/2}$ CF component. The superscript (1) indicates the CF component index. The tail of the curve is exponential with a decay time $\tau_{II} = 9.5$ ms. Coupling of the purely electronic transition to crystal lattice vibrations is observed via the occurrence of vibronic lines (figure 5). The strongest vibronic line is at ≈ 380 cm^{-1} from the zero-phonon line. This is a regular value for the phonon energy in a fluoride compound [9]. The ratio r_{II} of the integrated vibronic intensity to the integrated zero-phonon intensity amounts 0.05. Non-radiative transitions to the ground state can be neglected at 4.2 K and energy migration over the Gd^{3+} ions of class II to quenchers does not occur. We then have that the ratio r_{II} is equal to the ratio of the vibronic transition probability $A^{(1)}_{vib,II}$ and the zero-phonon transition probability $A^{(1)}_{zp,II}$ [12]. Here, the superscript indicates that these are values for the first CF component. The

subscript represents the class index. We find $A^{(1)}_{zp,II} = 100\ s^{-1}$ and $A^{(1)}_{vib,II} = 5\ s^{-1}$.

It is not possible to excite in such a way that only emission from class I is observed. To obtain the value of r for the $^6P_{7/2} \rightarrow {}^8S_{7/2}$ transition of Gd^{3+} in class I, we excite the sample at 35 845 cm^{-1}. We define R as the ratio of the zero-phonon intensities of classes II and I, and r_{I+II} as the ratio of the total vibronic intensity to the total zero-phonon intensity. The value of the integrated vibronic intensity to the integrated zero-phonon intensity occurring from class I is then given by $r_I = r_{I+II}(1+R) - r_{II}R$. This yields $r_I = 0.04$. The decay curve of the $^6P_{7/2} \rightarrow {}^8S_{7/2}$ transition of Gd^{3+} in class I also shows an initial build up. The exponential tail has a decay time of $\tau_I = 9.2$ ms.

The occurrence of energy transfer from class I to class II means that τ_I^{-1} equals the sum of the radiative transition probability, $A_{r,I} = A_{zp} + A_{vib}$, and the energy transfer transition probability, A_{I-II}. We note that the decay times of the $^6P_{7/2} \rightarrow {}^8S_{7/2}$ transition do not differ much for the both classes. For Gd^{3+} in a fluoride compound it is expected that this transition has only a magnetic dipole contribution (see later). The radiative transition probabilities are henceforth expected to be the same for both classes. Clearly, the extra decay path for class I by energy transfer to class II does not speed up the relaxation of class I considerably. The ratio of A_{I-II} to $A_{zp,I}$ equals the ratio of the total emission intensity of class II to the total emission intensity of class I (after excitation in one of the CF components of class I): $A_{I-II}/A_{zp,I} = R \cdot (1 + r_{II})/(1 + r_I)$. With $R = 0.26$ the radiative transition probabilities for the $^6P_{7/2} \rightarrow {}^8S_{7/2}$ transition of Gd^{3+} in class I are estimated to be $A^{(1)}_{zp,I} = 83\ s^{-1}$ and $A^{(1)}_{vib,I} = 3\ s^{-1}$. The energy transfer probability equals $A_{I-II} = 22\ s^{-1}$.

No vibronic lines are observed for the $^6I_{7/2} \rightarrow {}^8S_{7/2}$ transition. The decay time τ of this transition is 2.8 and 2.6 ms for classes I and II, respectively. The $^6I^{(1)}_{7/2}$ CF component decays via a radiative process to the $^8S_{7/2}$ ground state and via a non-radiative process to the ^6P_J term levels. After the non-radiative decay, the $^6P_{7/2} \rightarrow {}^8S_{7/2}$ transition takes place. For the $^6I^{(1)}_{7/2}$ CF component, therefore, τ^{-1} equals the sum of the radiative, $A^{(1)}_{zp}$, and non-radiative, $A^{(1)}_{nr}$, transition probability. For Gd^{3+} in class II an additional non-radiative decay route exists via energy transfer to Gd^{3+} in class I. This will be incorporated in the value of A_{nr}. The ratio of the $^6I_{7/2} \rightarrow {}^8S_{7/2}$ emission intensity to the $^6P_{7/2} \rightarrow {}^8S_{7/2}$ emission intensity yields the ratios of the radiative and non-radiative transition probabilities. The intensity ratio is measured as the density of photons. Thus we can derive the separate values of $A^{(1)}_{zp}$ and $A^{(1)}_{nr}$ for transitions starting from the $^6I^{(1)}_{7/2}$ term level, for both classes of sites. The values are given in table 1.

With increasing temperatures the higher CF components of the term levels are also observed in emission (figure 6). After excitation at 35 702 cm^{-1}, i.e. selective excitation of site II, and at temperatures above 25 K, the emission lines of site I are also observable (figure 6).

4. Discussion

From the emission spectra at 4.2 K, figures 1 and 2, we conclude that there are two different classes of site, I and II. To summarize the differences between the classes, we

note that the barycentre of the CF components is lowest and the CF splitting and the inhomogeneous broadening are largest for class II. The lower position of the barycentre means that sites in class II are the more covalent sites.

In the crystal structure we also distinguish two different classes of cation sites: (a) cation sites that are occupied either by a rare earth ion or by K^+ according to a fixed statistical distribution; and (b) sites that are occupied by a rare earth ion (Y^{3+} or Gd^{3+}). We now try to bring the spectroscopical and crystallographical classification into agreement. Therefore we note that in the first coordination sphere, cations in both classes are surrounded by F^- ions in a slightly distorted fluorite arrangement. In their second coordination sphere, cations in class (b) [(a)] have mainly cations in class (a) [(b)]. The statistical distribution of K^+ and rare earth ions over the sites in class (a) hence yields the more inhomogeneous environment for sites in class (b). Moreover, the presence of K^+ in class (a) increases the covalency of Gd^{3+} on a site in class (b). We thus conclude that class II corresponds to class (b) and that class (I) corresponds to class (a).

The assignment is confirmed by the emission spectrum at 4.2 K in the $^6P_{7/2} \rightarrow {}^8S_{7/2}$ transition region after low resolution excitation. For this, we first note that in a unit cell there are twelve rare earth ions belonging to class (b) and six rare earth ions in class (a) (see section 2.1). The radiative transition probabilities are of the same order of magnitude for the two classes. Therefore, the emission of Gd^{3+} in class II will be strongest after low resolution excitation, i.e. equal excitation intensity for both classes. We measured the emission spectrum in the $^6P_{7/2} \rightarrow {}^8S_{7/2}$ transition region on the MPF-44B spectrofluorometer. It is found that the class II emission has a larger intensity than the class I emission. This confirms that class (II) corresponds to class (b).

The positions of the $^6P_{7/2}$ and the $^6I_{7/2}$ term levels are in good agreement with positions found in other fluorides [7, 13, 14]. Vibronic lines are observed in the $^6P_{7/2} \rightarrow {}^8S_{7/2}$ transitions and are not observed in the $^6I_{7/2} \rightarrow {}^8S_{7/2}$ transition, in accordance with theory [15, 9]. The vibronic intensity ratios, r_I and r_{II}, and the transition probabilities are of a magnitude comparable with values found for $LaF_3 : Gd^{3+}$ and $LiYF_4 : Gd^{3+}$ [9].

The rare earth zero-phonon transitions have, in general, a forced electric-dipole (forced ED) and a magnetic-dipole contribution. The magnetic-dipole (MD) contribution to the $^6P_{7/2} \rightarrow {}^8S_{7/2}$ transition is 122 s^{-1} [16, 12]. The measured zero-phonon transition probability is even smaller than this value. Apparently, practically no ED contribution is present in the $^6P_{7/2} \rightarrow {}^8S_{7/2}$ transition. Since the sites have no inversion symmetry, this is ascribed to the high position of the opposite parity states ($\gtrsim$ 75 000 cm^{-1} [17]). Mixing of opposite parity configuration into the $^6P_{7/2}$ wavefunctions is therefore negligible. The theoretical value of 122 s^{-1} for the MD transition probability is the average value over the equally populated CF components. Our measured values are the probabilities from the lowest CF component. This may account for the difference between the theoretical value and our measured value. It cannot be excluded that the decay times are influenced by retrapping of emission in the crystal. If retrapping occurs, the true radiative transition probabilities will be slightly larger than the values presented here.

In order to measure the contributions of the other CF components, one should measure the intensity of the $^6P_{7/2}^{(\mu)} \rightarrow {}^8S_{7/2}$ zero-phonon transition relative to the intensity of the $^6P_{7/2}^{(1)} \rightarrow {}^8S_{7/2}$ zero-phonon transition as a function of temperature

[12, 9]. We could not do so, since the $^6P_{7/2}$ term levels of the two Gd^{3+} sites have a spectral overlap.

Above 25 K energy transfer also occurs from class II to class I (figure 6). An accurate analysis of this migration process is beyond the scope of this article.

In conclusion, we have studied the spectroscopy of KYF_4 doped with 5 at.% Gd^{3+}. Evidence is given that Gd^{3+} occupies two classes of sites in the crystal lattice. At 4.2 K energy transfer occurs from class I to class II. Above 25 K, energy transfer also occurs vice versa.

Acknowledgments

The investigations were partly supported by the Netherlands Foundation of Chemical Research (SON) with financial aid from the Netherlands Foundation for Advancement of Pure Research (NWO) and the Netherlands Foundation for Technical Research (STW).

References

[1] Meyer G 1982 *Prog. Solid State Chem.* **14** 141
[2] Greis O and Haschke J M 1982 *Handbook of the Physics and Chemistry of Rare Earths* vol 5, ed K A Gschneidner and L Eyring (Amsterdam: North-Holland)
[3] Rez I S 1986 *Sov. J. Quantum Electron.* **13** 2071
[4] Dubinskii M A, Khaidukov N M, Garipov I G, Dem'yanets L M, Naumov A K, Semashko V V and Malyuosov V A 1990 *J. Mod. Opt.* **37** 1355
[5] Aleonard S, Le Fur Y, Pontonnier L, Gorius N F and Roux M Th 1978 *Ann. Chim. Fr.* **3** 417
[6] Hahn T 1983 *International Tables of Crystallography* (Dordrecht: Reidel) p 499
[7] de Vries A J, Hazenkamp M F and Blasse G 1988 *J. Lumin.* **42** 275
[8] Meyerink A, Nuyten J and Blasse G 1989 *J. Lumin.* **44** 19
[9] Sytsma J, van Schaik W and Blasse G 1991 *J. Phys. Chem. Solids* **52** 419
[10] de Vries A J and Blasse G 1988 *J. Chem. Phys.* **88** 7312
[11] Bouazaoui M, Jacquier B, Linares C and Stręk W 1991 *J. Phys.: Condens. Matter* **3** 921
[12] Sytsma J, Imbusch G F and Blasse G 1990 *J. Chem. Phys.* **91** 1456 (erratum 1990 *J. Chem. Phys.* **92** 3249)
[13] Carnall W T, Goodman G L, Rajnak K and Rana R P 1989 *J. Chem. Phys.* **90** 3443
[14] Carnall W T, Crosswhite H and Crosswhite H M 1977 Energy level structure and transition probabilities of the trivalent lanthanides in LaF_3 *Argonne National Laboratory Report*
[15] Judd B R 1988 *Phys. Scr.* **21** 543
[16] Carnall W T, Fields P R and Rajnak K 1968 *J. Chem. Phys.* **49** 4412
[17] Szczurek T and Schlesinger M 1985 *Rare Earth Spectroscopy* ed B Jezowska-Trezbiatowska, J Legendziewicz and W Stręk (Singapore: World Scientific) p 325